

35 **Introduction**

36

37 Counterfeit medicines are more and more present since the last decade. This is mostly due to
38 the extension of the internet and the apparition of numerous fraudulent websites where
39 anyone can easily and anonymously buy prescription only medicines [1,2]. In developed
40 countries, the most popular counterfeit drugs are lifestyle medicines like the
41 phosphodiesterase type 5 (PDE-5) inhibitor drugs: sildenafil citrate (Viagra[®]), tadalafil
42 (Cialis[®]) and more recently vardenafil hydrochloride (Levitra[®]) [3].

43

44 The internationally recognized definition of a counterfeit medicine is the one of the World
45 Health Organization (WHO) [4]:

46 “A counterfeit medicine is one which is deliberately and fraudulently mislabelled with
47 respect to identity and/or source. Counterfeiting can apply to both branded and generic
48 products and counterfeit products may include products with the correct ingredients or
49 with the wrong ingredients, without active ingredients, with insufficient active
50 ingredient or with fake packaging.”

51 However, the most encountered illegal drugs in Belgium do not exactly correspond to this
52 definition because most of them do not copy the packaging and brand names of the genuine
53 products. This is why the classification proposed by the Dutch National Institute for Public
54 Health and the Environment (RIVM) [3] was applied. They make the distinction between
55 counterfeits, which appearance is in conformity with genuine medicines and imitations which
56 do not look like genuine (table1). In fact these imitations come in most cases from Asia
57 (mainly India and China) where they do not recognize European and American patent laws.
58 So they are legally manufactured in those countries but illegally imported in Europe.

59

60 Several techniques have been used for the analysis of erectile dysfunction drugs [5]. Among
61 these, colorimetry [6,7], TLC [8], NMR (¹H, ¹³C, ¹⁵N) [9], NMR (¹H, ²D DOSY ¹H) [10],
62 HPLC-UV [11], LC-ESI-MS-MS [12], extracted ion LC-MS/TOF [13], LC-DAD-CD [14].
63 For the specific detection of counterfeit drugs, spectroscopic techniques are preferred because
64 they are fast and need only a little sample preparation or no preparation at all. Raman
65 spectroscopy has been used to detect counterfeit Viagra[®] by de Veij et al. [15], counterfeit
66 Cialis[®] by Trefi et al. [10] Roggo et al. [16] used Raman spectroscopy for the identification of
67 pharmaceutical tablets and Vajna et al. [17] used Raman spectroscopy for the identification of
68 different manufacturing technologies. Vredembregt et al. [8] used the near infrared (NIR)

69 spectroscopy to check the homogeneity of a batch of genuine Viagra[®] and to screen for the
70 presence of sildenafil citrate. Storme-Paris et al. [18] and Chong et al. [19] also used the NIR
71 spectroscopy for the detection of counterfeit drugs and the identification of antibiotics
72 respectively. A comparison of NIR and Raman spectroscopy for the detection of counterfeit
73 Lipitor[®] has been realised by de Peinder et al. [20]. It has been demonstrated that NIR-
74 Chemical imaging was able to detect counterfeit medicines [21, 22, 23]. Finally, Maurin et al.
75 [24] permitted the prediction of the presence of sildenafil citrate and/or particular excipients
76 in counterfeit Viagra[®] by the mean of X-ray powder diffraction (XRD).

77
78 In this study, 55 counterfeit and imitations of Viagra[®], 9 genuine Viagra[®], 39 counterfeit and
79 imitations of Cialis[®] and 4 genuine Cialis[®] were analysed by Raman-, NIR- and FT-IR-
80 spectroscopy. It has been investigated which technique or combination of these techniques
81 was the best to (1) detect counterfeit Viagra[®] and counterfeit Cialis[®] and (2) to make clusters
82 in illegal medicines which can be useful for forensic investigations by authorities.

83

84 **1. Experimental**

85

86 *1.1. Samples*

87 The counterfeit and imitation tablets of Viagra[®] and Cialis[®] were donated by the Federal
88 Agency for Medicines and Health Products in Belgium (AFMPS/FAGG). They all come from
89 postal packs ordered by individuals via internet sites. All samples were delivered in blisters or
90 closed jars with or without packaging. All samples, once received, were stored at ambient
91 temperature and protected from light. The samples have been divided in groups according to
92 their visual aspect. Table 2 and 3 shows the groups of Viagra[®]-like and Cialis[®]-like samples
93 respectively.

94

95 Pfizer SA/NV (Belgium) kindly provided one batch of each different dosage of Viagra[®]
96 (25mg, 50mg, 100mg). Two other batches of each dosage were purchased in a local pharmacy
97 in Belgium.

98 Eli Lilly SA/NV (Benelux) kindly provided one batch of commercial packaging of Cialis[®]
99 (10mg and 20mg). Two other batches of Cialis[®] 20mg were purchased in a local pharmacy in
100 Belgium.

101

102 All references were delivered in closed blisters with packaging and were stored protected
103 from light at ambient temperature.

104

105 1.2. Instrumental

106 1.2.1. Raman spectroscopy

107 A RamanRxn1 spectrometer (Kaiser Optical Systems, Ann Arbor, MI, USA), equipped with
108 an air-cooled charge coupled device (CCD) detector (back-illuminated deep depletion design)
109 was used in combination with a fiber-optic non-contact probe to collect Raman spectra from
110 the core of the tablets. The laser wavelength during the experiments was the 785 nm line from
111 a 785 nm Invictus NIR diode laser. All spectra were recorded in the range of 0-3500 cm^{-1} with
112 a resolution of 4 cm^{-1} using a laser power of 400 mW. Data collection, data transfer, and data
113 analysis were automated using the HoloGRAMSTM (Kaiser Optical Systems, USA, version
114 2.3.5) data collection software, the HoloREACTTM (Kaiser Optical Systems, USA, version
115 2.3.5) reaction analysis and profiling software, the Matlab software (The Matworks, Natick,
116 MA, USA, version 7.7), and the Grams/AI-PLSplusIQ software (Thermo Fisher Scientific,
117 Waltham, MA, USA, version 7.02). Ten second exposures were used for spectral acquisition.
118 Spectra were collected at 3 locations per tablet. Spectra were preprocessed by baseline
119 correction (Pearson's method, [25]), mean centered and averaged before data-analysis.

120

121 1.2.2. NIR spectroscopy

122 Diffuse reflectance NIR spectra were collected per tablet using a Fourier-Transform NIR
123 spectrometer (Thermo Fisher Scientific, Nicolet Antaris II near-IR analyzer) equipped with an
124 InGaAS detector, a quartz halogen lamp and an integrating sphere, which was used for NIR
125 spectra collection from the tablets. Data analysis was done using Thermo Fisher Scientific's
126 Result software, SIMCA-P (Umetrics AB, Kinnelon, NJ, USA, version 11) and Matlab (The
127 Matworks, Natick, MA, USA, version 7.7). Each spectrum was collected in the 10000 – 4000
128 cm^{-1} region with a resolution of 16 cm^{-1} and averaged over 16 scans. All spectra were
129 preprocessed using standard normal variate transformation (SNV) and mean centered before
130 data-analysis. Each spectrum was performed on the core of the tablet.

131

132 1.2.3. FT-IR spectroscopy

133 A Spectrum 1000 (Perkin Elmer, Waltham, MA, USA) FT-IR spectrometer with a DTGS
134 detector was used. All spectra were recorded from the accumulation of 16 scans in 4000-400
135 cm^{-1} range with a 4 cm^{-1} resolution. Samples were prepared by compressing a 0.3% mixture

136 of pulverised tablet with spectral grade KBr (Merck, Germany). Three spectra of each sample
137 were obtained, normalized and averaged.

138 Once recorded, the spectra were normalized with the Spectrum software (Perkin Elmer,
139 Waltham, MA, USA, version 5.0.1.).

140

141 *1.3. Chemometrics*

142 *1.3.1. PCA*

143 PCA is a variable reduction technique, which reduces the number of variables by making
144 linear combinations of the original variables. These combinations are called the principal
145 components and are defined in such way that they explain the highest (remaining) variability
146 in the data and are by definition orthogonal.

147 The importance of the original variables in the definition of a principal component is
148 represented by its loading and the projections of the objects on to the principal components
149 are called the scores of the objects. [26] In this investigation, it was decided to conduct the
150 research only on the three first PC's, since in all cases more than 95% of the variation in the
151 data was explained by them.

152

153 *1.3.2. PLS*

154 PLS is based on exactly the same principles as PCA. The difference is situated in the
155 definition of the latent variables, here called PLS-factors. The PLS-factors, also linear
156 combinations of the original explanatory variables in the data set, are defined in such a way
157 that they maximize the covariance with the response variable. In this way latent variables are
158 obtained that are more directly related to the response variable than, for example, those
159 obtained in PCA. In this study, a discrete response variable was chosen (0 for illegal samples
160 and 1 for genuine samples). This is justified since the genuinity of the reference samples is
161 certified.

162 The scores of the objects on the different PLS-factors were used in this study as tool to
163 distinguish clusters of the different samples. [26]

164

165 *1.3.3. Data processing*

166 The data pre-processing was performed using HoloREACT™ software. For NIR and FT-IR
167 spectroscopy, the three spectra of a sample were normalized and averaged. For Raman
168 spectroscopy, the three spectra of a sample were baseline corrected using the Pearson's
169 method. All calculations were done with Matlab (The Matworks, Natick, MA, version 7.9.0).

170 The Principal component analysis (PCA) of the data has been performed with algorithms
171 based on Kernel PCA [27]. The Partial Least Squares (PLS) analysis of the data has been
172 performed with the algorithms described by de Jong [28]. The algorithms are part of the
173 ChemoAC toolbox (Freeware, ChemoAC Consortium, Brussels, Belgium, version 4.0). For
174 each method, the dataset consist of a matrix with a number of columns equal to the number of
175 wavelengths measured and a number of rows equal to the number of samples studied. The
176 combination of the techniques has been performed by addition of the matrixes obtained for
177 each technique. The combination matrix was then autoscaled in order to eliminate the
178 influence of the differences of scaling.

179

180 **2. Results and Discussion**

181

182 *2.1. Measurements*

183 All IR measurements were performed in triplicate on the pulverised tablet. All NIR
184 measurements were performed once on the core of three different tablets of each sample and
185 all Raman measurements were performed on three different locations of the core of one tablet
186 of each sample. Only the fingerprint region of the IR spectra ($1800\text{-}400\text{ cm}^{-1}$) and the 7000-
187 4000 cm^{-1} region of the NIR spectra were used because of their high variability and their
188 richness of information. The Raman spectra were taken with an exposure time of ten seconds
189 on the core of the tablets at three different locations per tablet.

190

191 *2.2. Case one: Viagra[®]*

192 *2.2.1. PCA*

193 First, a PCA analysis was performed. No separation or not enough separation was seen
194 between genuine and counterfeit or imitation samples. FT-IR provided the best results for the
195 PCA analysis. It was decided to perform a PLS analysis. This choice was based on the
196 supervised character of this chemometric method.

197

198 *2.2.2. PLS*

199 *2.2.2.1. FT-IR spectroscopy*

200 Figure 1 shows the three dimensional PLS plot of the analysis of the FT-IR spectra of the
201 Viagra[®]-like samples. As can be seen, a good distinction between genuine and counterfeit or
202 imitations is obtained. Previous inspection of the loading plots confirms that almost the
203 complete fingerprint region is needed for classification. Most of the separation is probably

204 due to the differences in chemical composition of the tablets: combinations of different API,
205 differences in excipients used, presence of contaminants or both of them.

206 The counterfeit samples are quite close to each other (cluster 1) except two of them. Cluster
207 one contains also 4 imitations; this indicates that their chemical composition is presumably
208 similar to the one of the counterfeits. Among the different clusters identified, cluster 3 is very
209 far from the other ones (along the axes PLS 2 and PLS 3 on figure 2). No reason has been
210 identified for that huge separation. But it can be observed that cluster 3 is always separated
211 from other samples by each technique or combination of techniques except for Raman
212 spectroscopy and the combination of Raman and FT-IR spectroscopy. Clusters 4 and 5 can
213 easily be confirmed by visual examination. Each cluster contains tablets originating from the
214 same manufacturer. Cluster 2 contains two samples visually different but having the same
215 packaging (same brand name and dosage: Nizagara 25mg). The fact that these two samples
216 are close to each other indicates that they probably have the same chemical composition. They
217 may be manufactured in two different laboratories but with the same raw material.

218 Other samples are widespread and no relationship between these samples is seen. After
219 inspection of the loading plots, no specific wavenumbers corresponding to an excipient or the
220 sildenafil were correlated to the separation.

221

222 2.2.2.2. *NIR spectroscopy*

223 Figure 2 shows the three dimensional PLS plot of the analysis of the NIR spectra of the
224 Viagra[®]-like samples. As with FT-IR, a good separation between genuine and imitations or
225 counterfeit is obtained. Some clusters are observed. No obvious reason has been found as an
226 explanation of these clusters except for clusters 4 and 5. NIR cluster 4 contains the same
227 samples as the FT-IR cluster 5 and these samples are from the same manufacturer. NIR
228 cluster 5 contains chewing tablets of three different manufacturers. Their classification in the
229 same cluster is probably the consequence of a same manufacturing process. This is in line
230 with the principle of NIR spectroscopy which is dependant of the physical properties of the
231 sample such as particle size, density and morphology [29]. After visual inspection of the NIR
232 spectra, it appears that the major variability is present between 5500-5000 cm^{-1} .

233 After plotting the loadings in function of the wavenumbers (Fig 3a), it has been found that the
234 separation in groups by PLS factor 1 was due to microcrystalline cellulose (4732 cm^{-1}),
235 sodium laurylsulfate (5130 cm^{-1}) and sildenafil citrate (5250 cm^{-1}) (fig 3b). The separation by
236 PLS factor 2 was due to cellulose derivatives (5180 cm^{-1}) (fig 4 and 3b). The whole spectrum

237 was taken into account for the separation by PLS factor 3. It can therefore be postulated that
238 there are differences in the chemical composition of the tablets.

239

240 2.2.2.3. *Raman spectroscopy*

241 Raman spectroscopy was able to distinguish genuine from illegal medicines (fig 5). Illegal
242 samples were widespread and no cluster has been identified except two samples that are apart
243 from other ones. One of these two samples may be separated from other ones because it
244 contains both sildenafil and tadalafil.

245 No satisfying explanation has been found for the separation of the other sample and the
246 loading plots don't give more information.

247 The Raman spectra also have been evaluated in smaller spectral regions, but the conclusions
248 were similar.

249

250 2.2.2.4. *Combination of techniques.*

251 The association of Raman and FT-IR spectroscopy and the association of Raman and NIR
252 spectroscopy allow the distinction of 5 and 6 clusters respectively (results not shown). No
253 reason has been found for this distinction. Neither the visual aspect nor the loading plots
254 permits an explanation.

255 Fig 6 shows the three dimensional PLS plot of the analysis of the combination of the NIR and
256 FT-IR spectra of the Viagra[®] samples. A good separation between genuine and counterfeit or
257 imitation samples can be observed. The illegal samples are divided in 4 clusters. These
258 clusters are the most relevant for a forensic investigation because the classification realised by
259 the combination of the two techniques shows clusters that are the most different according to
260 both physical and chemical properties. These differences should be relatively little among
261 samples from the same manufacturer. Cluster 3 contains the same samples as cluster 3 in Fig
262 1 and 2. Cluster 4 contains some samples from group 2 and 4 (see table 2). Samples from
263 group 2 are all manufactured by Axon Drugs Pvt Ltd. No reason has been found for the
264 presence of samples from group 4 because no manufacturer name was present. They may be
265 manufactured by Axon Drugs but this can not be confirmed. No satisfying reason has been
266 found to explain the cluster 2. Once again, no specific wavenumbers corresponding to an
267 excipient of the genuine tablets or the sildenafil were correlated to the separation according to
268 the loading plots.

269 Once Raman spectroscopy data are introduced in the analysis, clusters are no more coherent
270 with the visual aspect of the tablets. As it cannot be ruled about the relevance of the

271 information provided by the Raman spectroscopy, the combination of NIR and FT-IR
272 spectroscopy will be preferred.

273

274 2.3. Case two: *Cialis*[®]

275 2.3.1. *PCA*

276 As for *Viagra*[®], the PCA analysis of Raman spectroscopy didn't allow to distinguish genuine
277 from imitations or counterfeit samples. So this technique was abandoned to the advantage of
278 NIR and FT-IR.

279 PCA analysis of the *Cialis*[®] FT-IR dataset (fig 7) permitted to clearly separate the counterfeit
280 samples (cluster 2 in figures 7 and 8) from the imitations and from the genuine samples.
281 Cluster 3 contains the remaining samples. However, a group of imitations is not separated
282 from genuine samples (cluster 1 in figures 7 and 8). The same observation is done with the
283 NIR dataset (Fig 8). The imitations (group 5 in table 3) have different brand names but are
284 visually similar and can be easily identified as being only one group. The qualitative and
285 quantitative analysis by HPLC and dissolution of some of them indicates that they are of good
286 quality. This might result of a chemical composition and a manufacturing process very close
287 to the original *Cialis*[®]. So, the PLS analysis was needed to distinguish these imitations from
288 the originals.

289 The samples of clusters 4 are coherent with visual inspection. Cluster 3 and 5 in figure 8
290 cannot formally be explained. Cluster 2 contains the counterfeit samples.

291

292 2.3.2. *PLS*

293 2.3.2.1. *FT-IR spectroscopy*

294 The PLS analysis permitted a very good separation of the imitations and the counterfeits from
295 the genuine samples. FT-IR also permitted to see 5 clusters of samples (fig 9). Cluster 1
296 shows the imitations samples that weren't separated from the genuine samples by PCA. It
297 contains imitations that are visually similar: oval shape with E20 embossed; without
298 distinction between conventional tablets and chewable tablets (see table 3). It can therefore be
299 postulated that only few chemical differences are present (flavouring agents such as menthol).
300 After qualitative and quantitative HPLC analysis and according to the classification of the
301 RIVM [3], they can be called "professional imitations".

302 Cluster 2 contains the counterfeit samples. It is very clearly separated from other samples. A
303 HPLC analysis showed that they contain both sildenafil and tadalafil. So they can be called
304 "mixed counterfeit" according to the RIVM classification [3]. This combination of API may

305 explain this clear separation. Cluster 3 contains samples from the same manufacturer
306 (according to the packaging) that are visually similar: round, orange and without film-coat. In
307 this case, the chewable tablets were separated from other samples (arrow 3).

308 Cluster 4 contains samples that are neither counterfeit nor imitation samples. Their packaging
309 is totally different from genuine samples but their shape, film-coat colour and engraving C20
310 are similar. However, they really seem manufactured by amateurs so we classed them among
311 imitations. Once again, the chewable version of these tablets is not comprised in the cluster
312 (arrow 4).

313 Cluster 5 contains the other samples except three of them that are widespread in the plot.
314 They are not similar between them but quite close to each other. They probably have the same
315 chemical composition and the same manufacturer.

316 The examination of the loading plots did not permit to identify which component was
317 correlated with this separation. After visual inspection of the FT-IR spectra of each cluster, it
318 can be observed that almost the whole spectrum is different between each sample except
319 between cluster one and genuine samples which is in agreement with the fact that they
320 weren't separated by PCA.

321

322 2.3.2.2. *NIR spectroscopy*

323 NIR spectroscopy shows a clear separation between genuine samples and counterfeit or
324 imitation ones (fig 10). Clusters 1 and 2 are very clearly separated from other samples but the
325 clustering of the illegal samples is not clear (clusters 3, 4). These 2 clusters are very close to
326 each other. Once again, the counterfeit samples (cluster 2) are clearly separated from other
327 samples. The visual inspection of the NIR spectra of each cluster shows no clear difference
328 between the different clusters.

329

330 2.3.2.3. *Raman spectroscopy*

331 Raman spectroscopy permits the distinction between genuine and illegal samples. This
332 distinction was greater when the region between 1400-1190 cm^{-1} was studied. So this region
333 has been selected for the rest of the analysis with Raman spectroscopy on Cialis[®]-like
334 samples. Figure 11a shows the separation of the illegal samples in 3 clusters. Cluster 1
335 contains the imitations from the group 5 (see table 3) and one sample from the group 7. This
336 sample wasn't classified in any cluster by both NIR and FT-IR spectroscopy. Cluster 3
337 contains two samples from the same group but no reason has been found for their separation
338 from the other ones. The loading plots didn't permit to identify which component was

339 correlated with these clusters. As shown on figure 11b, the Raman spectra of the three clusters
340 are different in particular in the studied region (grayed area).

341

342 2.3.2.4. *Combination of techniques.*

343 The NIR and the FT-IR data were associated to obtain figure 12. This plot shows a separated
344 cluster of the genuine samples and four other clusters. Cluster 1 contains the professional
345 imitations identified by both FT-IR and NIR (group 5 of table 3) and it contains also a sample
346 that was not included in a cluster by each technique separately except by the Raman
347 spectroscopy. Cluster 2 contains the counterfeit samples and cluster 3 contains the remainder
348 samples. Only one sample stand alone (cluster 4), this sample was included in cluster 5 by
349 both techniques separately (fig 9 and 10). It couldn't be explained why the association of the
350 techniques isolated it.

351 Figure 13 shows the combination of the NIR and the Raman spectra. Three clusters are
352 observed. These clusters are the same as for the association of NIR and FT-IR spectroscopy
353 except that the sample from group 7 that was in cluster one is now separated in cluster 5. The
354 sample of cluster 4 in fig 12 is still isolated.

355 Figure 14 shows the association of the FT-IR and the Raman spectra. This time, illegal
356 samples are divided into 4 clusters. Clusters 2 and 3 are coherent with visual inspection of the
357 tablet. Cluster 4 contains all the samples from group 3 except a tablet from group 4. This
358 sample was already classified close to group 3 by FT-IR spectroscopy (see fig 9). Cluster 1
359 contains the remainder samples.

360 The association of the three techniques permitted exactly the same separation as the
361 association of NIR and Raman spectroscopy.

362

363 **3. Conclusion**

364 The aim of this study was to establish which technique or combination of techniques was the
365 most powerful to distinguish counterfeits from genuine samples of Viagra[®] and Cialis[®]. The
366 spectroscopic techniques investigated comprised FT-IR, NIR and Raman spectroscopy.

367 FT-IR is a widely spread and relatively cheap technique, used for decades and present in each
368 analytical laboratory. The main drawback of this technique is its destructive character.

369 NIR and Raman techniques are more and more used in the pharmaceutical industry because of
370 their easiness of use, their rapidity and the fact that it is non-destructive. So, any further
371 analysis can still be done on the tablets analysed by NIR or Raman spectroscopy which is
372 very important for an official analytical laboratory.

373

374 The ability of NIR and Raman spectroscopy separately to make the distinction between
375 genuine and counterfeit or imitation samples has already been demonstrated [8,10,15]. PCA
376 analysis of the data was insufficient to achieve complete separation of the samples. Hence,
377 PLS analysis was preferred because it is a powerful tool for a discrimination study with
378 reference samples.

379 For the Viagra[®] samples, after investigation, the conclusion is that the association of NIR and
380 FT-IR spectroscopy provides the best results (see table 4a). Indeed, the many clusters
381 observed with NIR and FT-IR alone were reduced to 4 clusters showing the most variability
382 between the samples. This variability is correlated to both physical and chemical information.
383 This is very useful for a forensic investigation because it takes into account both chemical
384 composition and the manufacturing process. This information is useful for characterizing a
385 manufacturer.

386 For the Cialis[®]-like samples, each technique separately permitted a classification of the
387 samples and the distinction between genuine and illegal samples (see table 4b). But this
388 classification was insufficient for the Raman spectroscopy or incomplete for the FT-IR and
389 the NIR spectroscopy. It is concluded that the association of NIR spectroscopy (region
390 between 7000-4000 cm⁻¹) and Raman spectroscopy (region between 1400-1190 cm⁻¹) was the
391 most useful association of techniques. This association permitted a very good separation
392 between genuine and counterfeit or imitation samples. The classification performed allows the
393 distinction between very bad counterfeits, very good imitations and other samples from
394 genuine samples. This classification is also very easy even by visual inspection of a non-
395 trained operator. This is useful for its application in control laboratory. The association of FT-
396 IR and Raman spectroscopy has not been considered as optimal because some groups were
397 not separated and there were samples misclassified. For these reasons, this association seems
398 to be less useful than the association of NIR and Raman spectroscopy.

399 This study was performed on a limited number of samples. If those techniques are applied to a
400 routine forensic laboratory working on counterfeit drugs, it is clear that the constitution of a
401 library of genuine and illegal samples would allow a sharper classification of samples.

402 The use of spectroscopic tools allows an objective distinction between legal and illegal tablets
403 based on chemical and physical information of the tablets. This distinction sometimes
404 confirms the visual classification of the samples but most of the time it completes this
405 classification. As it has been demonstrated, it is frequent that many visually similar samples
406 are finally classified in the same cluster which indicates that they have similar physico-

407 chemical properties. That kind of objective classification is the most useful for any further
408 investigation.

409

410 **4. References**

411

412 [1] A. Weiss, Buying prescription drugs on the internet: promises and pitfalls, Cleveland
413 Clinic Journal of Medicine 73 (2006), 3, 282-288

414 [2] M. Veronin, B.-B. Youan, Magic bullet gone astray: medications and the internet, Science
415 305 (2004), 5683, 481

416 [3] B.J. Venhuis, D.M. Barends, M.E. Zwaagstra, D. de Kaste, Recent developments in
417 counterfeit and imitations of Viagra, Cialis and Levitra, RIVM Report 370030001/2007,
418 Bilthoven, 2007

419 [4] WHO, sixty-second world health assembly item 12.9, counterfeit medical products, April
420 2009. http://aps.who.int/gb/ebhwa/pdf_files/A62/A62_13-en.pdf

421 [5] S. Singh, B. Prasad, A. Savaliya, R.P. Shah, V.M. Gohil, A. Kaur, Strategies for
422 characterizing sildenafil, vardenafil, tadalafil and their analogues in herbal dietary
423 supplements, and detecting counterfeit products containing these drugs, Trends in Analytical
424 Chemistry 28 (2009), 1, 13-28

425 [6] A.S. Amin, M.E. Moustafa, R. El-Dosoky, Colorimetric determination of sildenafil citrate
426 (Viagra) through ion-associate complex formation, Journal of AOAC International 92(2009),
427 1, 125-130

428 [7] A.L. Rodomonte, M.C. Gaudiano, E. Antoniella, D. Lucente, V. Crusco, M. Bartolomei,
429 P. Bertocchi, L. Manna, L. Valvo, N. Muleri, Counterfeit drugs detection by measurement of
430 tablets and secondary packaging colour, Journal of Pharmaceutical and Biomedical Analysis
431 (2010), doi:10.1016/j.jpba.2010.03.044

432 [8] M.J. Vredenbregt, L. Blok-Tip, R. Hoogerbrugge, D.M. Barends, D. de Kaste, Screening
433 suspected counterfeit Viagra and imitations of Viagra with near-infrared spectroscopy,
434 Journal of Pharmaceutical and Biomedical Analysis 40 (2006), 4, 840-849

435 [9] I. Wawer, M. Pisklak, Z. Chilmonczyk, ¹H, ¹³C, ¹⁵N NMR analysis of sildenafil base
436 and citrate (Viagra) in solution, solid state and pharmaceutical dosage forms, Journal of
437 Pharmaceutical and Biomedical Analysis 38 (2005), 5, 865-870

438 [10] S. Trefi, C. Routaboul, S. Hamieh, V. Gilard, M. Malet-Martino, R. Martino, Analysis of
439 illegally manufactured formulations of tadalafil (Cialis) by ¹H NMR, 2D DOSY ¹H NMR
440 and Raman spectroscopy, Journal of Pharmaceutical and Biomedical Analysis 47 (2008), 1,
441 103-113









442 [11] H.Y. Aboul-Enein, I. Ali, Determination of tadalafil in pharmaceutical preparation by
443 HPLC using monolithic silica column, Talanta 65 (2005), 1, 276-280.

- 444 [12] M.J. Bogusz, H. Hassan, E. Al-Enazi, Z. Ibrahim, M. Al-Tufail, Application of LC-ESI-
445 MS-MS for detection of synthetic adulterants in herbal remedies, *Journal of Pharmaceutical*
446 *and Biomedical Analysis* 41 (2006), 2, 554-564
- 447 [13] A.A. Savaliya, R.P. Shah, B. Prasad, S. Singh, Screening of Indian aphrodisiac
448 ayurvedic/herbal healthcare products for adulteration with sildenafil, tadalafil and/or
449 vardenafil using LC/PDA and extracted ion LC-MS/TOF, *Journal of Pharmaceutical and*
450 *Biomedical Analysis* 52 (2010), 3, 406-409
- 451 [14] B.J. Venhuis, G. Zomer, M.J. Vredenburg, D. de Kaste, The identification of (-)-trans-
452 tadalafil, tadalafil, and sildenafil in counterfeit Cialis and the optical purity of tadalafil
453 stereoisomers, *Journal of Pharmaceutical and Biomedical Analysis* 51 (2010), 3, 723-727
- 454 [15] M. de Veij, A. Deneckere, P. Vandenaabeele, D. de Kaste, L. Moens, Detection of
455 counterfeit Viagra with Raman spectroscopy, *Journal of Pharmaceutical and Biomedical*
456 *Analysis* 46 (2008), 2, 303-309
- 457 [16] Y. Roggo, K. Degardin, P. Margot, Identification of pharmaceutical tablets by Raman
458 spectroscopy and chemometrics, *Talanta* 81 (2010), 3, 988-995
- 459 [17] B. Vajna, I. Farkas, A. Szabó, Z. Zsigmond, G. Marosi, Raman microscopic evaluation
460 of technology dependent structural differences in tablets containing imipramine model drug,
461 *Journal of Pharmaceutical and Biomedical Analysis* 51 (2010), 5, 30-38
- 462 [18] I. Storme-Paris, H. Rebiere, M. Matoga, C. Civade, P.-A. Bonnet, M.H. Tissier, P.
463 Chaminade, Challenging near infrared spectroscopy discriminating ability for counterfeit
464 pharmaceuticals detection, *Analytica Chimica Acta* 658 (2010), 2, 163-174
- 465 [19] X.-M. Chong, C.-Q. Hu, Y.-C. Feng, H.-H. Pang, Construction of a universal model for
466 non-invasive identification of cephalosporins for injection using near-infrared diffuse
467 reflectance spectroscopy, *Vibrational Spectroscopy* 49 (2009), 196-203
- 468 [20] P. de Peinder, M.J. Vredenburg, T. Visser, D. de Kaste, Detection of Lipitor
469 counterfeits: a comparison of NIR and Raman spectroscopy in combination with
470 chemometrics, *Journal of Pharmaceutical and Biomedical Analysis* 47 (2008), 4-5, 688-694
- 471 [21] T. Puchert, D. Lochmann, J.C. Menezes, G. Reich, Near-infrared chemical imaging
472 (NIR-CI) for counterfeit drug identification--a four-stage concept with a novel approach of
473 data processing (Linear Image Signature), *Journal of Pharmaceutical and Biomedical*
474 *Analysis* 51 (2010), 1, 138-145
- 475 [22] M.B. Lopes, J.C. Wolff, Investigation into classification/sourcing of suspect counterfeit
476 Heptodintrade mark tablets by near infrared chemical imaging, *Analytica Chimica Acta* 633
477 (2009), 1, 149-155

- 478 [23] M.B. Lopes, J.C. Wolff, J.M. Bioucas-Dias, M.A. Figueiredo, Determination of the
479 composition of counterfeit Heptodin tablets by near infrared chemical imaging and classical
480 least squares estimation, *Analytica Chimica Acta* 641 (2009), 1-2, 46-51
- 481 [24] J.K. Maurin, F. Pluciński, A.P. Mazurek, Z. Fijałek, The usefulness of simple X-ray
482 powder diffraction analysis for counterfeit control--the Viagra example, *Journal of*
483 *Pharmaceutical and Biomedical Analysis* 43 (2007), 4, 1514-1518
- 484 [25] G.A. Pearson, A general baseline-recognition and baseline-flattening algorithm. *Journal*
485 *of Magnetic Resonance* 27 (1977), 2, 265–272.
- 486 [26] D.L. Massart, B.G.M. Vandeginste, L.M.C. Buydens, S. De Jong, P.J. Lewi, J.Smeyers-
487 verbeke: *Handbook of Chemometrics and Qualimetrics-Part A*. Elsevier Science, Amsterdam,
488 1997
- 489 [27] W. Wu, D.L. Massart, S. de Jong, The kernel PCA algorithms for wide data. Part I:
490 Theory and algorithms, *Chemometrics and Intelligent Laboratory Systems* 36 (1997), 2, 165-
491 172
- 492 [28] S. de Jong, SIMPLS: An alternative approach to partial least squares regression,
493 *Chemometrics and Intelligent Laboratory Systems* 18 (1993), 251-263
- 494 [29] G. Reich, Near-infrared spectroscopy and imaging: Basic principles and pharmaceutical
495 applications, *Advanced Drug Delivery Reviews* 57 (2005), 1109-1143
496







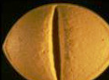


Main category	Subcategory	Inclusion and exclusion criteria
Counterfeit	Professional	Appearance in conformity with genuine medicine; Content of correct API within 90 - 110 % of declared value; No other APIs; not genuine medicine.
	Non-professional	Appearance in conformity with genuine medicine; Content of correct API outside 90 - 110 % of declared value; No other APIs.
	Mixed	Appearance in conformity with genuine medicine; Contains correct API and another, known API
	Fraudulent	Appearance in conformity with genuine medicine; Contains a different, known API.
	Analog	Appearance in conformity with genuine medicine, Contains other, unapproved API
	Placebo	Appearance in conformity with genuine medicine; Does not contain APIs.
Imitation	Professional	Appearance not in conformity with genuine medicine; Content of correct API within 90 - 110 % of declared value; No other APIs.
	Non-professional	Appearance not in conformity with genuine medicine; Content of declared API outside 90 - 110 % of declared value; No other APIs.
	Mixed	Appearance not in conformity with genuine medicine; Contains declared API and another API.
	Fraudulent	Appearance not in conformity with genuine medicine; Contains an undeclared API.
	Analog	Appearance not in conformity with genuine medicine; Contains other, unapproved API
	Placebo	Appearance not in conformity with genuine medicine; Does not contain APIs.

501 Table 2 : Viagra[®]-like samples. (For RIVM classes see table 1)
 502

Group number	Sample photo	Symbol in plots	RIVM Class	Number of Samples
1		•	Non-professional counterfeits	6
2		X	Professional imitation	8
3		□	Professional imitations and one non-professional imitation	4
4		*	Professional imitation	23
5		△	Professional imitation	4
6		☆	Professional imitation and one mixed imitation	5
Other		◇	Non-professional imitation and one professional imitation	5
genuine		○		9

503
 504

505 Table 3: Cialis[®]-like samples. (For RIVM classes see table 1)
 506

Group number	Sample photo	Symbol in plots	RIVM Class	Number of samples
1		•	Mixed counterfeits	5
2		X	Professional imitation	4
3		□	Professional imitation	5
4		*	Non-professional imitation	3
5		△	Professional imitation	13
6		☆	Non-professional imitation and two mixed imitations	4
7		☆	Non-professional imitation	2
other		◇	Professional imitation and mixed imitations	3
genuine		○		4

507
 508
 509

510 Table 4: (a) Summary table of the results obtained with the different techniques and
 511 associations analysed by PLS for the Viagra[®]-like samples. The best method is in bold font.
 512

Viagra[®]-like samples	Genuine discrimination	Counterfeit-Imitations discriminations	Clusters number	Explained clusters	Unclassified samples
FT-IR (1800-400cm ⁻¹)	Yes	No	5	4	33
NIR (7000-4000 cm ⁻¹)	Yes	No	5	2	31
Raman (1800-200cm ⁻¹)	Yes	No	-	-	55
FT-IR+NIR	Yes	No	4	2	0
FT-IR+Raman	Yes	No	5	1	2
NIR+Raman	Yes	No	6	1	2
FT-IR+NIR+Raman	Yes	No	6	1	2

513 (b) Summary table of the results obtained with the different techniques and
 514 associations analysed by PLS for the Cialis[®]-like samples. The best method is in bold font.
 515
 516

Cialis[®]-like samples	Genuine discrimination	Counterfeit-Imitations discriminations	Clusters number	Explained clusters	Unclassified samples
FT-IR (1800-400cm ⁻¹)	Yes	Yes	5	4	3
NIR (7000-4000cm ⁻¹)	Yes	Yes	5	4	3
Raman (1400-1190cm ⁻¹)	Yes	Yes	3	2	1
FT-IR+NIR	Yes	Yes	3	2	1
FT-IR+Raman	Yes	Yes	4	3	0
NIR+Raman	Yes	Yes	3	2	2
FT-IR+NIR+Raman	Yes	Yes	3	2	2

517
 518
 519

520 Fig 1: 3D PLS score plot of the FT-IR spectra (region between 1800-400cm⁻¹) of the
521 Viagra[®]-like samples. For symbol caption see table 2.

522

523 Fig 2: 3D PLS score plot of the NIR spectra (region between 7000-4000cm⁻¹) of the Viagra[®]-
524 like samples. For symbol caption see table 2.

525

526 Fig 3: (a) Loadings scores of the PLS 1 of the NIR spectra of the Viagra[®]-like samples.
527 Three major peaks are observed at 4732, 5130 and 5250 cm⁻¹.

528 (b) NIR spectra of the excipients linked to the peaks identified in (a).

529

530 Fig 4: Loadings scores of the PLS 2 of the NIR spectra of the Viagra[®]-like samples. The
531 major peak observed is at 5180 cm⁻¹. This wavenumber can be linked to the cellulose
532 derivatives excipients.

533

534 Fig 5: 3D PLS score plot of the Raman spectra (region between 1800-200cm⁻¹) of the
535 Viagra[®]-like samples. For symbol caption see table 2.

536

537 Fig 6: 3D PLS score plot of the association of the FT-IR spectra (region between 1800-400
538 cm⁻¹) and the NIR spectra (region between 7000-4000 cm⁻¹) of the Viagra[®]-like samples. For
539 symbol caption see table 2.

540

541 Fig 7: 3D PCA score plot of the FT-IR spectra (region between 1800-400cm⁻¹) of the
542 Cialis[®]-like samples. For symbol caption see table 3.

543

544 Fig 8: 3D PCA score plot of the NIR spectra (region between 7000-4000cm⁻¹) of the Cialis[®]-
545 like samples. The results show no separation of genuine samples. For symbol caption see
546 table 3.

547

548 Fig 9: 3D PLS score plot of the FT-IR spectra (region between 1800-400cm⁻¹) of the Cialis[®]-
549 like samples. For symbol caption see table 3.

550

551 Fig 10: 3D PLS score plot of the NIR spectra (region between 7000-4000cm⁻¹) of the Cialis[®]-
552 like samples. For symbol caption see table 3.

553

554 Fig 11:(a) 3D PLS score plot of the Raman spectra (region between 1400-1190 cm^{-1}) of the
555 Cialis[®]-like samples. For symbol caption see table 3.

556 (b) Mean Raman spectrum of each cluster. The region between 1400-1190 cm^{-1} is
557 grayed.

558

559 Fig 12: 3D PLS score plot of the association of the FT-IR spectra (region between 1800-400
560 cm^{-1}) and the NIR spectra (region between 7000-4000 cm^{-1}) of the Cialis[®]-like samples. For
561 symbol caption see table 3.

562

563 Fig 13: 3D PLS score plot of the association of the Raman spectra (region between 1400-1190
564 cm^{-1}) and the NIR spectra (region between 7000-4000 cm^{-1}) of the Cialis[®]-like samples. For
565 symbol caption see table 3.

566

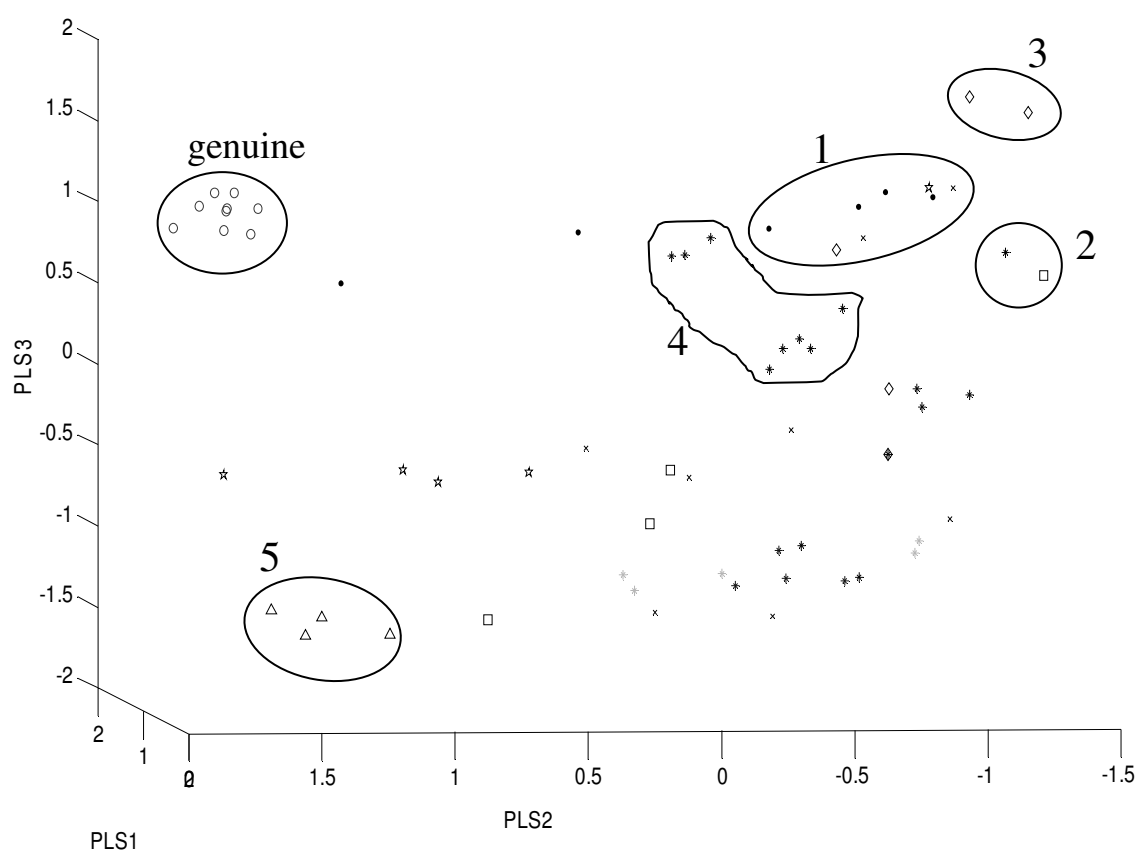
567 Fig 14: 3D PLS score plot of the association of the FT-IR spectra (region between 1800-400
568 cm^{-1}) and the Raman spectra (region between 1400-1190 cm^{-1}) of the Cialis[®]-like samples.

569 For symbol caption see table 3.

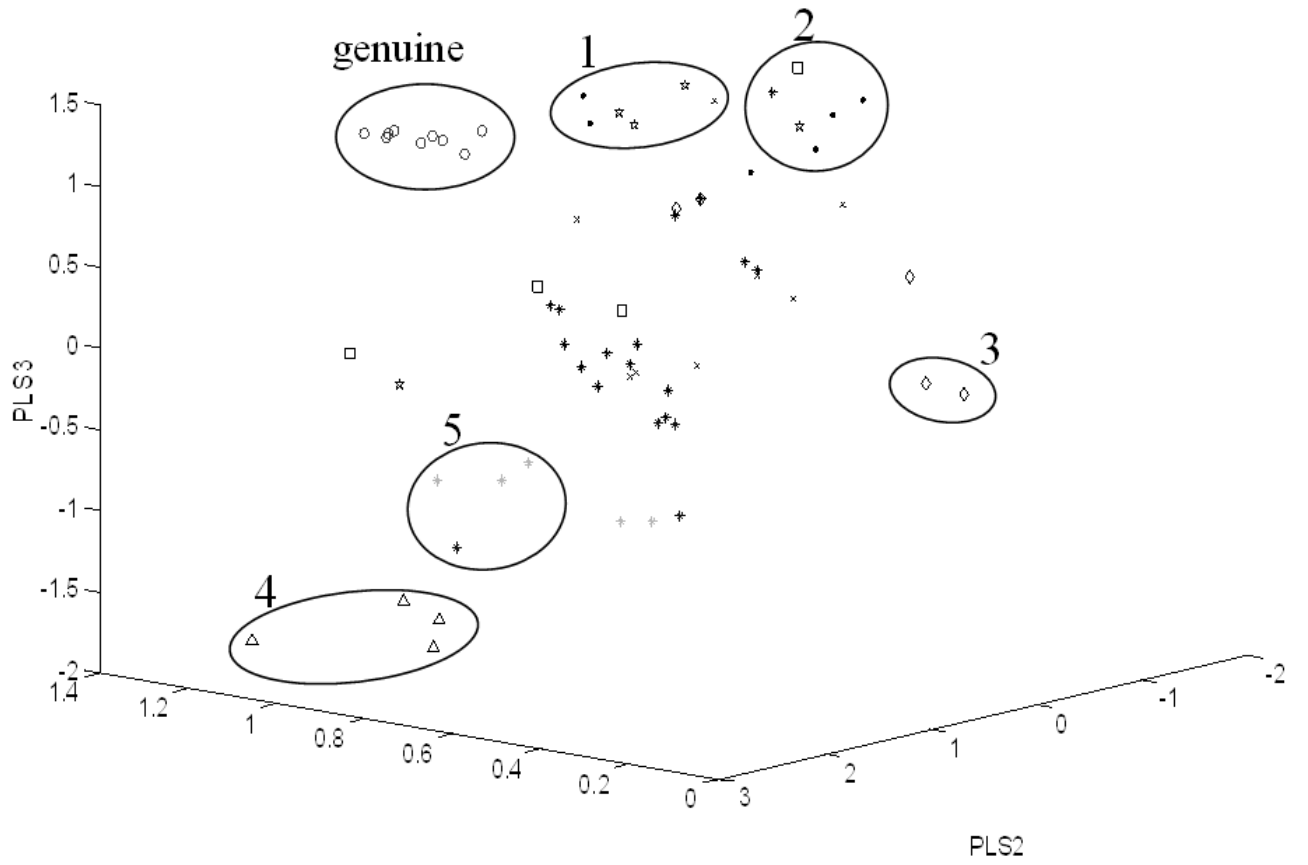
570

571 Fig 1

572
573
574
575
576
577
578
579
580
581
582
583
584
585
586
587
588
589
590
591
592
593
594
595
596
597
598
599
600
601
602
603
604
605
606
607
608
609
610
611
612
613
614
615
616
617
618
619
620

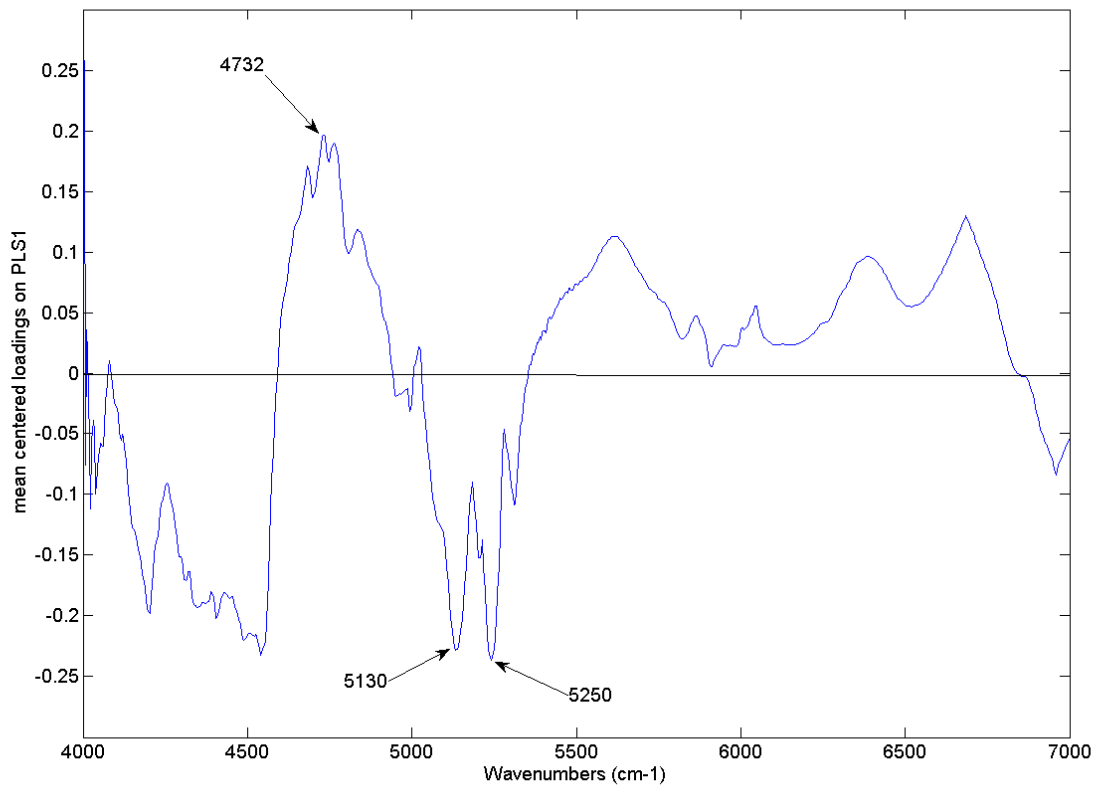


621 Fig 2:

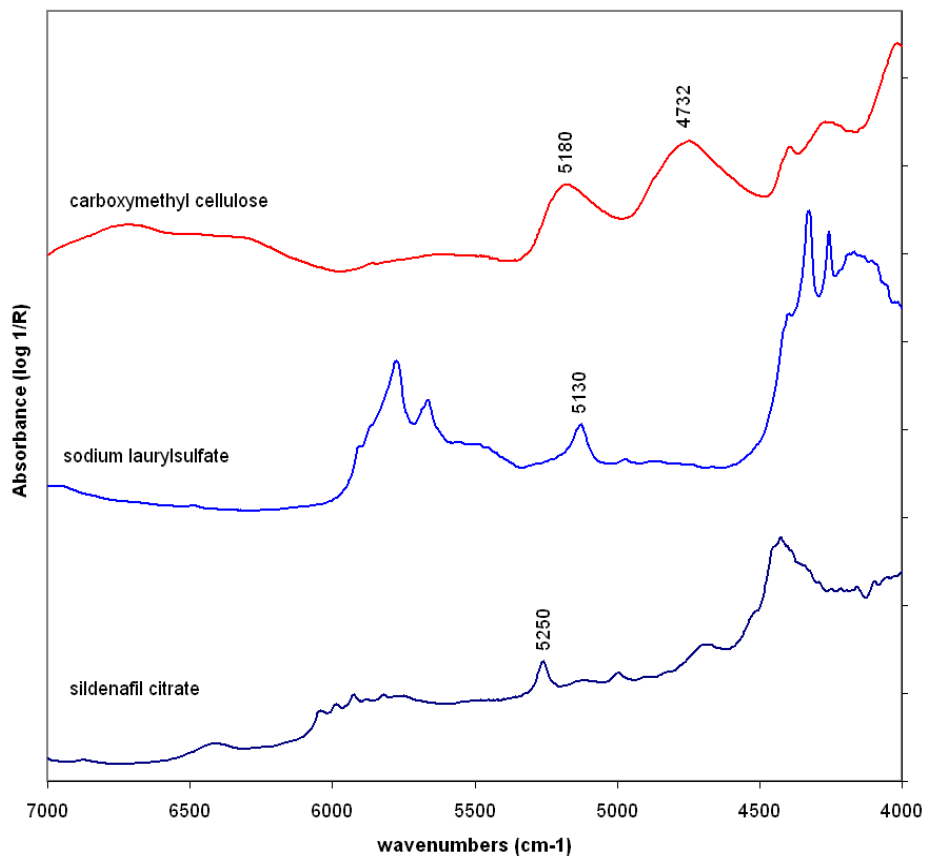


622
623
624
625
626
627
628
629
630
631
632
633
634
635
636
637
638
639
640
641
642
643
644
645
646

647 Fig 3a:

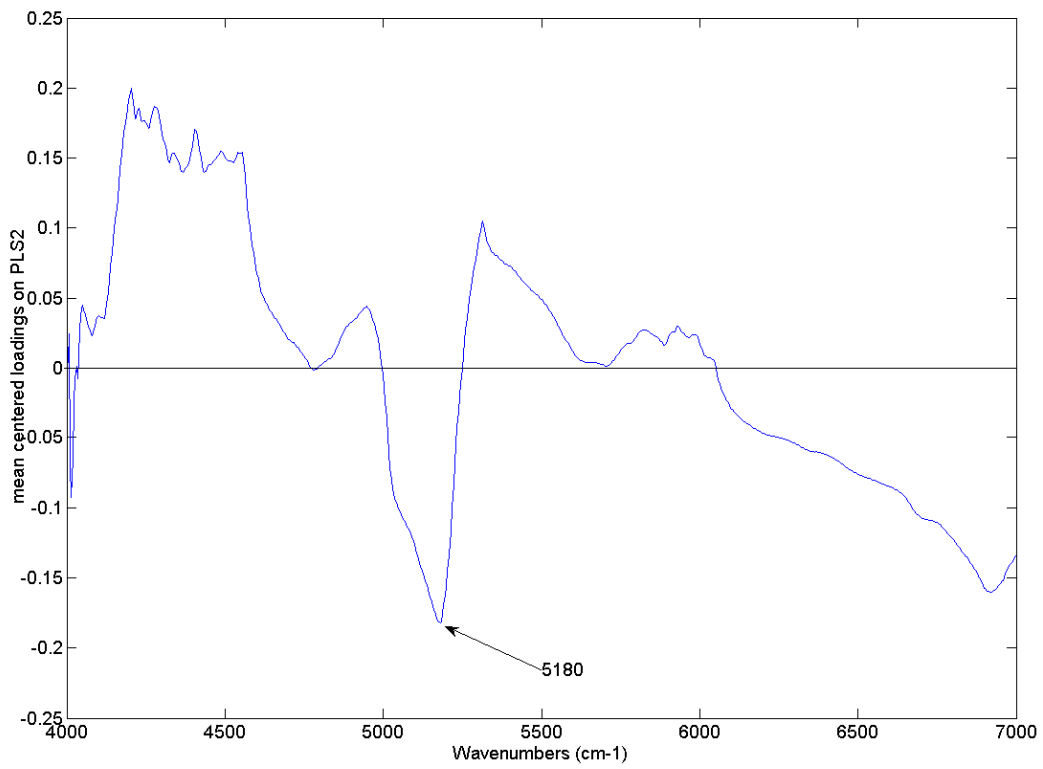


648
649 Fig 3b:



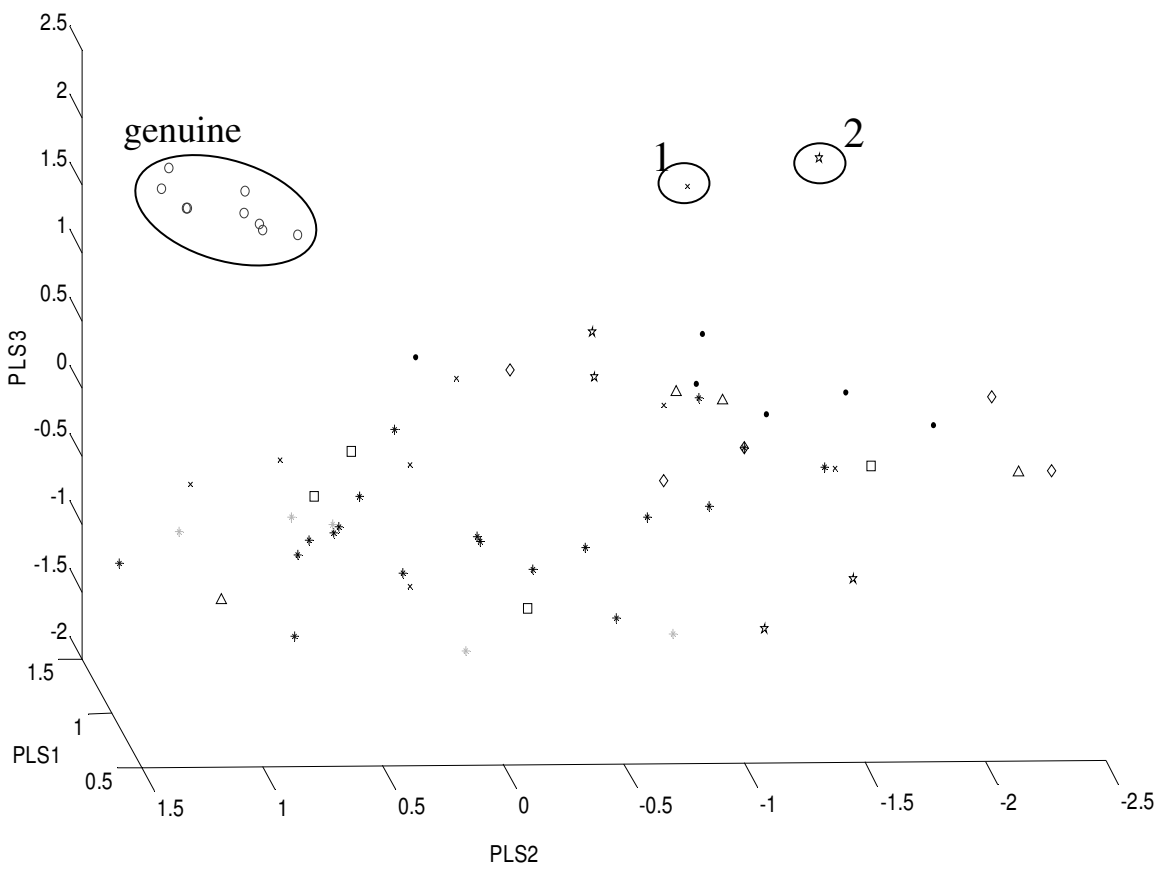
650
651
652
653
654
655
656
657
658
659
660
661
662
663
664
665
666
667
668
669
670
671
672
673

674 Fig 4:



- 675
- 676
- 677
- 678
- 679
- 680
- 681
- 682
- 683
- 684
- 685
- 686
- 687
- 688
- 689
- 690
- 691
- 692
- 693
- 694
- 695
- 696
- 697
- 698
- 699

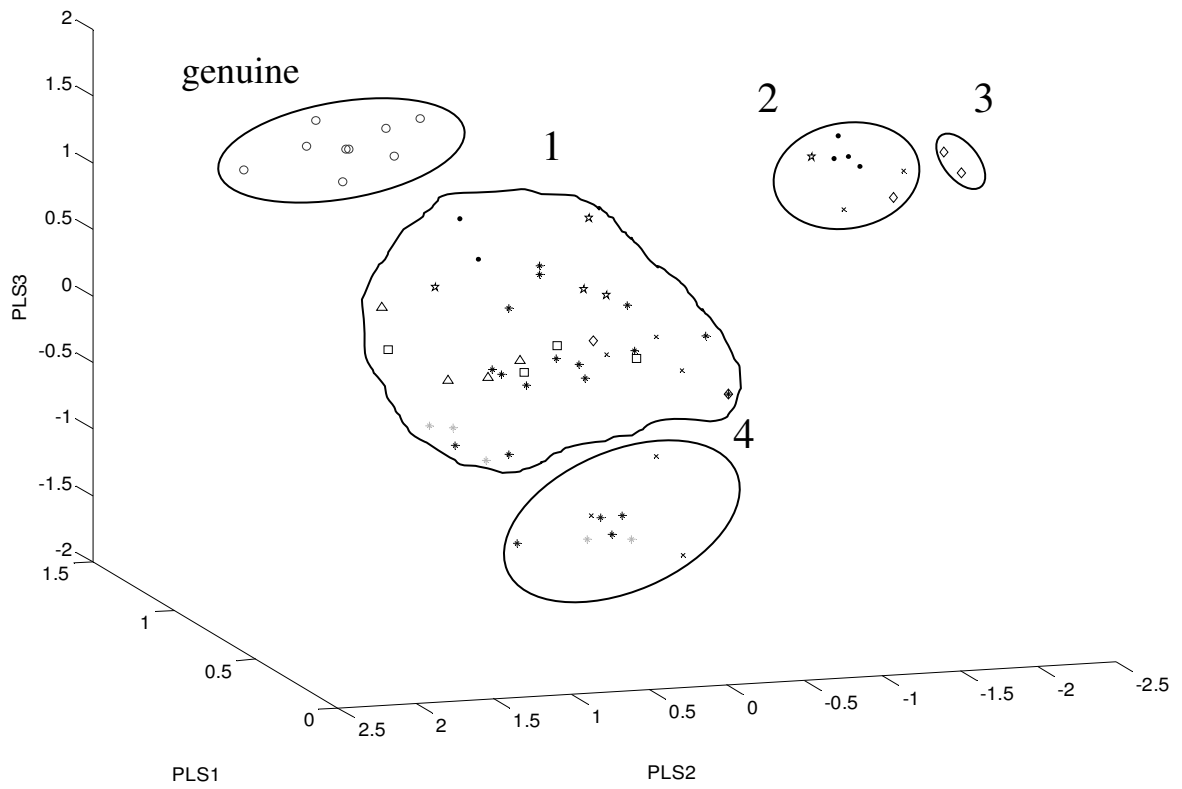
700 Fig 5:



701
702
703
704
705
706
707
708
709
710
711
712
713
714
715
716
717
718
719
720
721
722
723
724
725
726
727
728
729
730
731
732
733
734
735
736
737
738
739
740
741
742
743
744
745
746
747
748
749

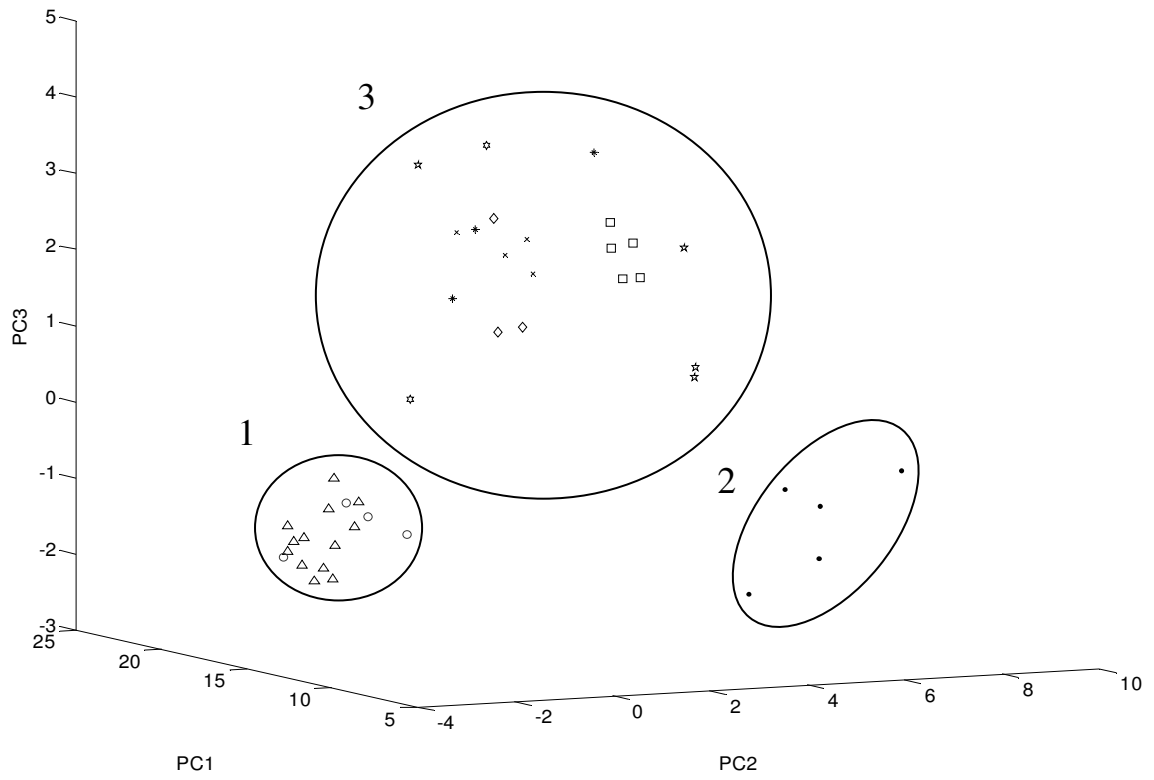
750 Fig 6:

751
752
753
754
755
756
757
758
759
760
761
762
763
764
765
766
767
768
769
770
771
772
773
774
775
776



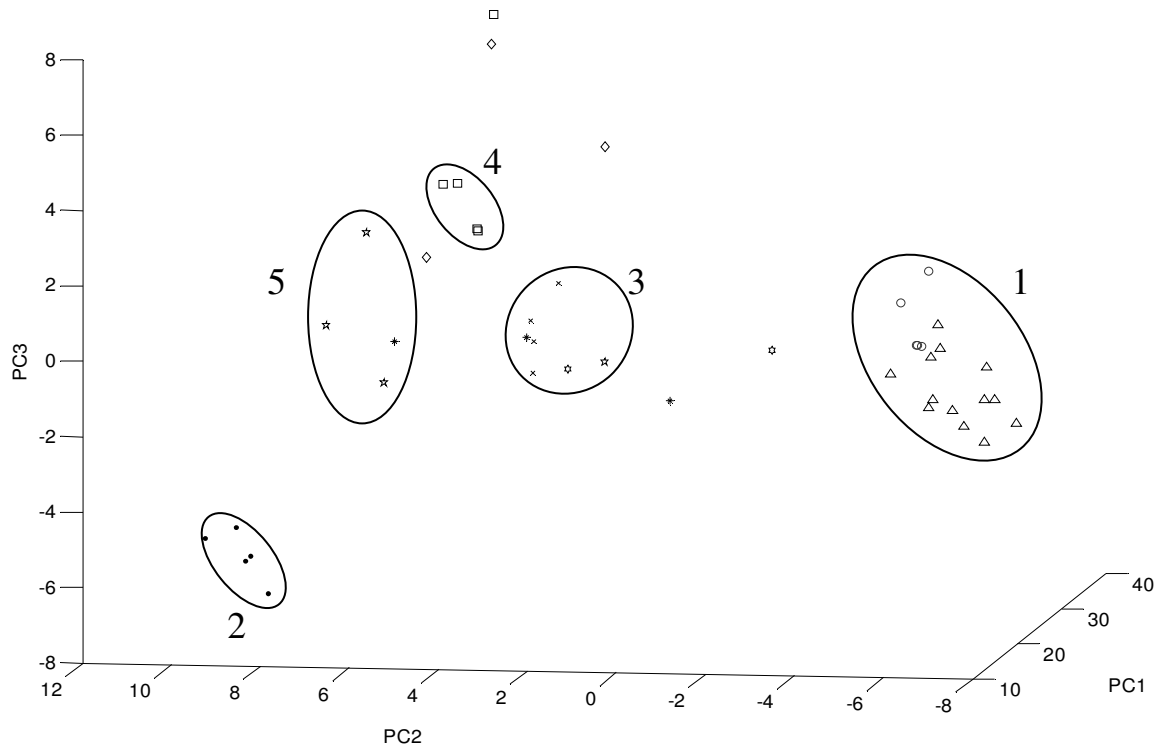
777 Fig 7:

778
779
780
781
782
783
784
785
786
787
788
789
790
791
792
793
794
795
796
797
798



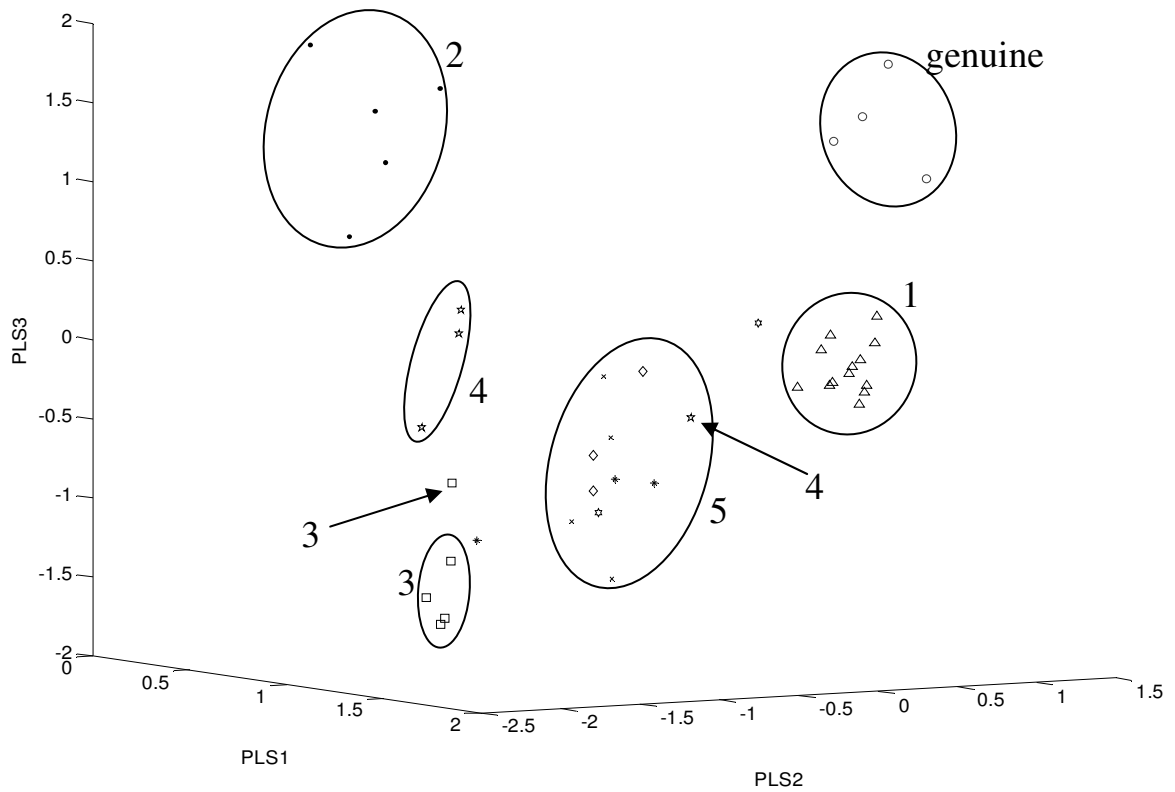
799 Fig 8:

800
801
802
803
804
805
806
807
808
809
810
811
812
813
814
815
816
817
818
819
820
821
822
823
824
825



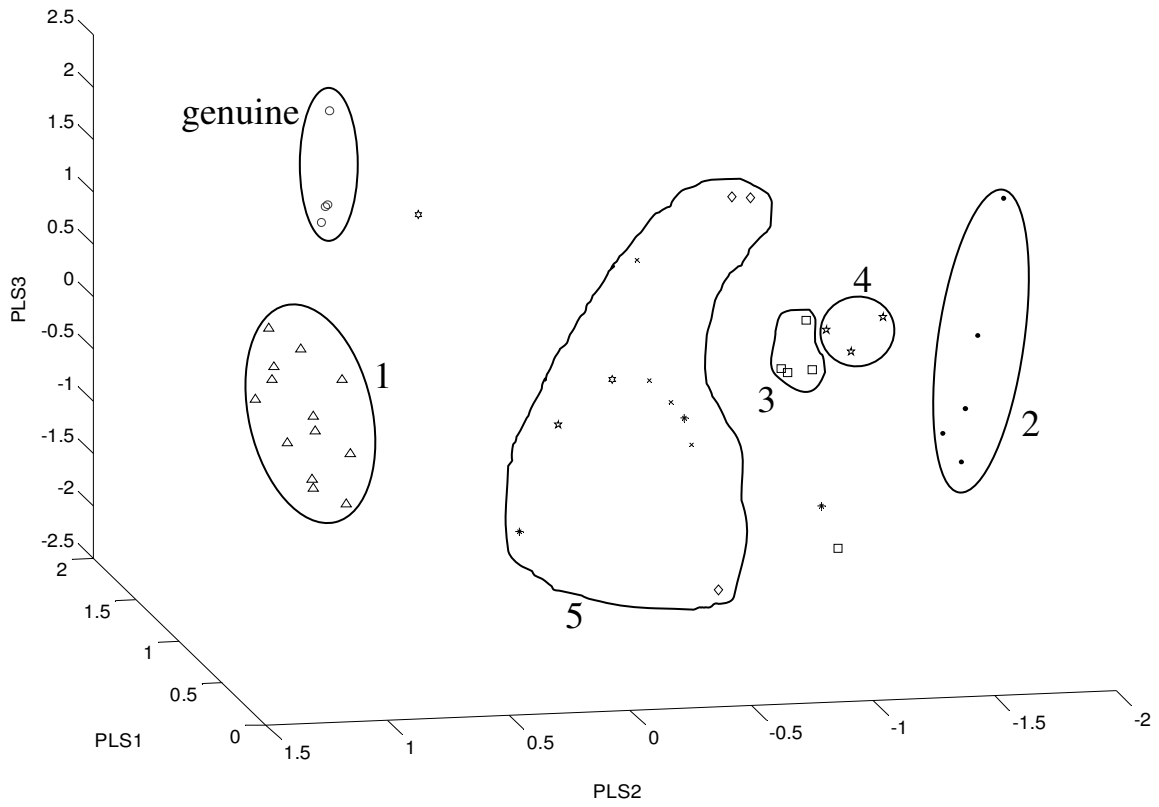
826 Fig 9:

827
828
829
830
831
832
833
834
835
836
837
838
839
840
841
842
843
844
845
846
847
848
849
850
851
852
853
854
855
856
857
858
859
860
861
862
863
864
865
866
867
868
869
870
871
872
873
874
875

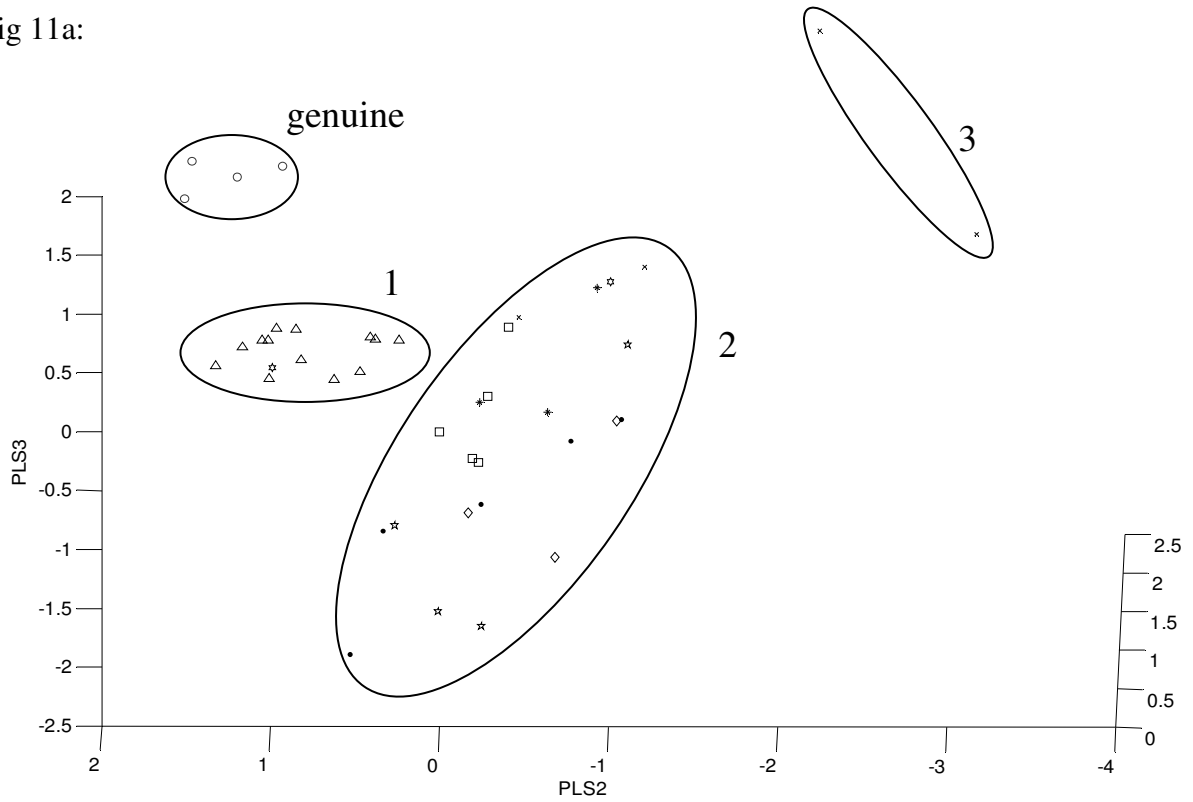


876 Fig 10

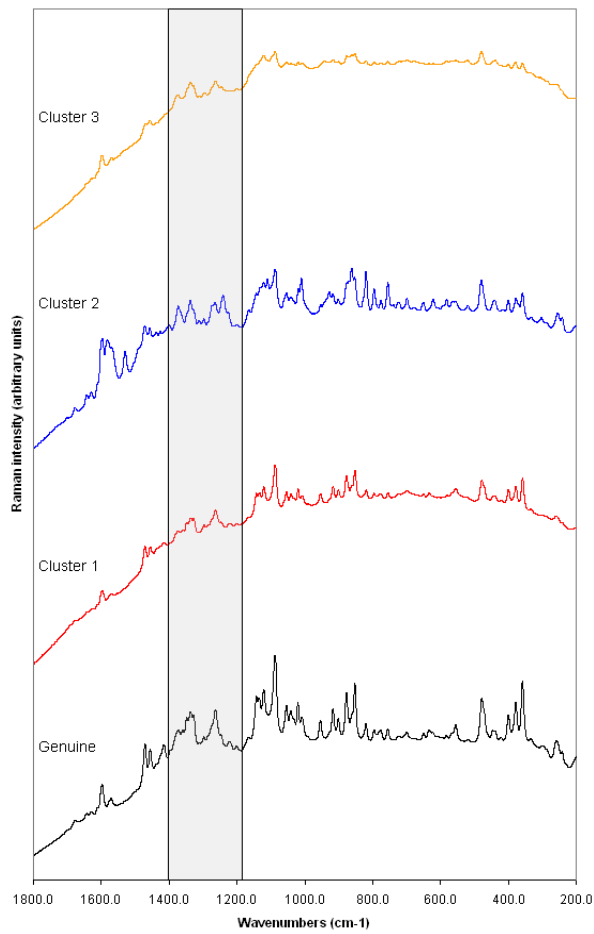
877
878
879
880
881
882
883
884
885
886
887
888
889
890
891
892
893
894
895
896
897
898
899
900
901
902
903
904
905
906
907
908
909
910
911
912
913
914
915
916
917
918
919
920
921
922
923
924
925



926 Fig 11a:



948 Fig 11b:



976 Fig 12:

977

978

979

980

981

982

983

984

985

986

987

988

989

990

991

992

993

994

995

996

997

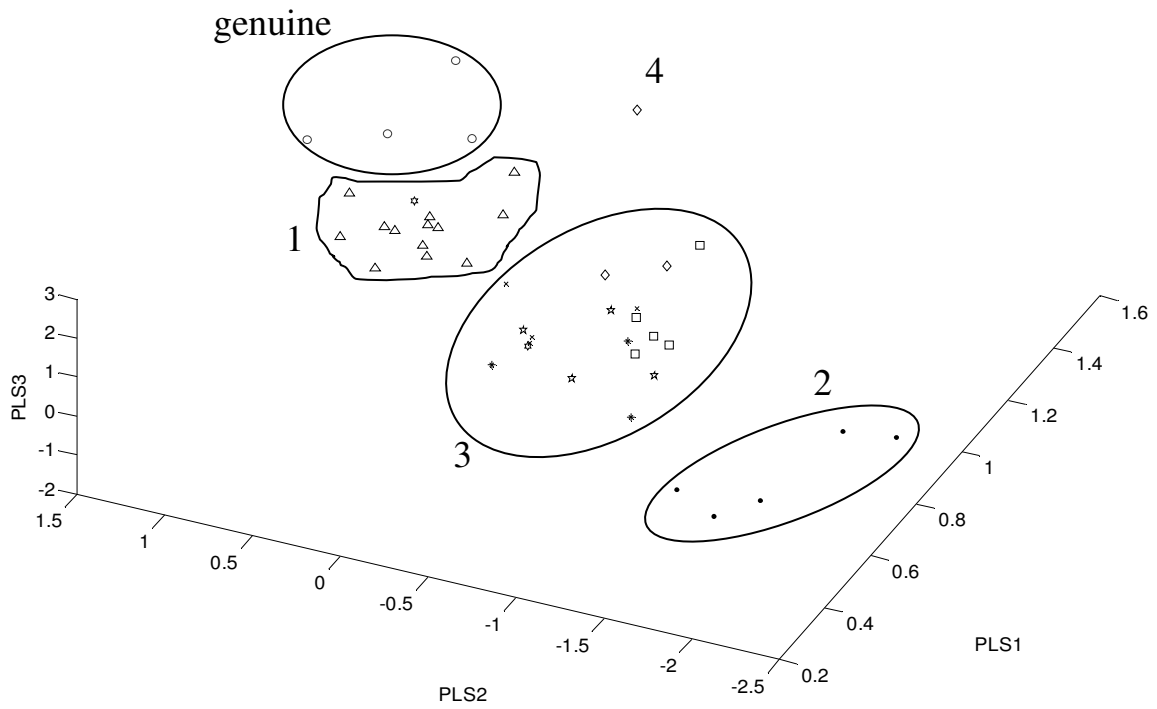
998

999

1000

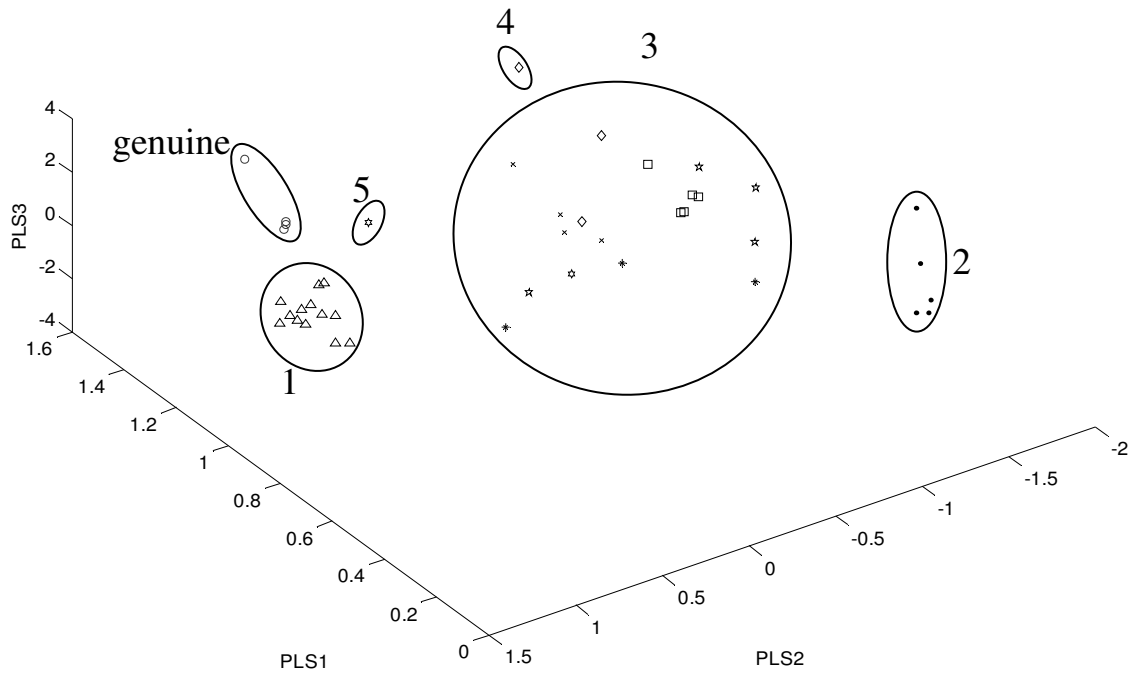
1001

1002



1003 Fig 13:

1004
1005
1006
1007
1008
1009
1010
1011
1012
1013
1014
1015
1016
1017
1018
1019
1020
1021
1022
1023
1024
1025
1026
1027



1028 Fig 14:

1029
1030
1031
1032
1033
1034
1035
1036
1037
1038
1039
1040
1041
1042
1043
1044
1045
1046
1047
1048
1049
1050
1051
1052
1053
1054
1055

